Astronomy & Astrophysics manuscript no. output
January 12, 2024

Tidal frequency dependence of the Saturnian Love number k_2

V. Lainey[1], J. Dewberry[2], J. Fuller[3], N. Cooper[4], N. Rambaux[1], and Q. Zhang[5]

[1] IMCCE, Observatoire de Paris, PSL Research University, CNRS, Sorbonne Université, Univ. Lille
e-mail: valery.lainey@obspm.fr
[2] CITA, 60 St. George Street, Toronto, ON M5S 3H8, Canada
[3] TAPIR, Mailcode 350-17, California Institute of Technology, Pasadena, CA 91125, USA
[4] Department of Physics Astronomy, Queen Mary University of London, Mile End Rd, London E1 4NS, UK
[5] Department of Computer Science, Jinan University, Guangzhou 510632, PR China

ABSTRACT

Context. Love numbers describe the elastic response of a body to the gravitational action of another massive object. By quantifying these numbers, we can better model the interior of the celestial objects concerned.
Aims. In the present work, we determine Saturn's degree-2 Love number, k_2, at four different frequencies.
Methods. To do this, we use astrometric data from the Cassini spacecraft and a dynamical model of the orbits of Saturn's moons.
Results. The values obtained are equal to ... for the tidal frequencies of Janus/Epimetheus, Mimas, Tethys and Dione.
Conclusions. We show that these values are compatible with a constant Love number. In addition, we compare the observed values with a model of inertial waves excited in Saturn's interior, and obtain good agreement.

Key words. –Planets and satellites: interiors – Astrometry –

1. Introduction

Among the most surprising results obtained with the Cassini probe concerning the orbital dynamics of the moons, we can easily cite the quantification of tidal effects on Saturn. Using thousands of astrometric data from NAC camera images, (Lainey et al. 20 ??) were able to highlight the strong orbital expansion of the moons. This is characterized to first order by the tidal ratio k2/Q, where k_2 is the Love number of degree 2 and Q is the quality factor characterizing the dissipation of tidal energy in the planet. Using the motion of the four coorbital moons of Tethys and Dione, Lainey et al. (2017) were even able to independently quantify the two parameters k_2 and Q. In a later work, Lainey et al. (2020) even managed to quantify the quality factor Q at six different frequencies, corresponding to the tidal frequencies raised by Mimas, Enceladus, Tethys, Dione, Rhea and Titan.

In the present work, we have investigated whether it is also possible to quantify Saturn's Love number at different tidal frequencies. Using all the astrometric data currently available, we show that it can be quantified at four tidal frequencies associated with the action of the moons Janus and Epimetheus, Mimas, Tethys and Dione. We then compare the results obtained with the values predicted by modelling the inertial modes present in the planet.

In section 2, we present the dynamical modeling used, as well as the fitting of the orbital model to astrometric data from the Cassini probe. In section 3, we briefly present how Saturn's interior was modeled, and compare the results obtained from astrometry with our model.

2. Orbital fit

We carried out orbital dynamical modelling and fitting to the observations in a similar way to Lainey et al. (2023) and Lainey et al. (2024), with the additional improvement of solving for an independent k_2 for each tide raisin moons frequency. The gravity harmonics were still solved for, but were constrained to remain in agreement with the solution of Iess et al. (2019), within their given uncertainty. For convenience, we review our method and the relevant equations below, and refer the reader to Lainey et al. (2023) and Lainey et al. (2024) for further details.

2.1. Dynamical modelling

Using the NOE gravitational N-body code (Lainey et al. 2007), we fitted the full equations of motion (see equation (1)) to the astrometric observations available (see subsection 2.2), solving for the initial positions, velocities of the eight main moons, the four coorbitals Telesto, Calypso, Helen and Polydeuces, the four inner moons Atlas, Prometheus, Pandora, Janus, and the small moons Methone, Anthe and Pallene. In addition, global parameters, such as the masses, C_{np} and S_{np} gravity coefficients, and Saturnian polar orientation were simultaneously solved for. Following (Lainey et al. 2023), the physical librations of Prometheus, Pandora, Janus, and Epimetheus were considered, also. Last the Love number for each tide raising moon ws solved for, together with a supposedly constant Love number k_3.

Our model included (i) gravitational interactions up to degree 2 in the expansion of the gravitational potential of the satellites (Table 2 from (Lainey et al. 2019)) and degree 10 for Saturn (Iess et al. 2019); (ii) gravitational perturbations between all moons; (iii) the solar perturbation (where the masses of the inner planets and the Moon were incorporated into the solar mass), and Jupiter based on the DE430 ephemeris; (iv) the precession of Saturn;

(v) tidal effects based on the Love numbers k_2 and k_3, neglecting dissipation; and (vi) relativistic corrections.

Following Lainey et al. (2007), the equation of motion for a satellite P_i may be expressed as

$$\begin{aligned}\ddot{\mathbf{r}}_i &= -G(m_0+m_i)\left(\frac{\mathbf{r}_i}{r_i^3} - \nabla_i U_{\bar{i}\hat{0}} + \nabla_0 U_{\bar{0}\bar{i}}\right)\\ &+ \sum_{j=1,j\neq i}^{\mathcal{N}} Gm_j\left(\frac{\mathbf{r}_j-\mathbf{r}_i}{r_{ij}^3} - \frac{\mathbf{r}_j}{r_j^3} + \nabla_j U_{\bar{j}\hat{0}} - \nabla_0 U_{\bar{0}\hat{j}} - \nabla_j U_{\bar{j}\bar{i}} + \nabla_i U_{\bar{i}\bar{j}}\right)\\ &+ \frac{(m_0+m_i)}{m_i m_0}\mathbf{F}^T_{\bar{i}\hat{0}} + \sum_{j=1,j\neq i}^{N}\left(-\frac{\mathbf{F}^T_{\bar{j}\hat{0}}}{m_0} + \frac{\mathbf{F}^T_{ij}}{m_i}\right) + GR, \qquad (1)\end{aligned}$$

where $\mathbf{r}_i$ and $\mathbf{r}_j$ are the position vectors of the satellite P_i and a perturbing body P_j (another satellite, the Sun, or Jupiter) with mass m_j, respectively, subscript 0 denotes Saturn, $U_{\bar{k}\bar{l}}$ is the gravity field of body P_l at the position of body P_k (including planetary oblateness), GR are corrections due to general relativity (Newhall et al. 1983), $\mathbf{F}^T_{\bar{l}\hat{0}}$ is the force on P_l from the tides it raises on its primary body, and $\mathbf{F}^T_{ij}$ is the effect of tides raised by one moon on Saturn acting on another moon. In the absence of tidal dissipation, the latter two forces are given by Lainey et al. (2007, 2017):

$$\mathbf{F}^T_{\bar{l}\hat{0}} = -\frac{3k_2 Gm^2 (E_r)^5 \mathbf{r}_l}{r_l^8}, \qquad (2)$$

$$\mathbf{F}^T_{ij} = \frac{3k_2 Gm_j m_i R^5}{2r_i^5 r_j^5}\left[-\frac{5(\mathbf{r}_i\cdot\mathbf{r}_j)^2\mathbf{r}_i}{r_i^2} + r_j^2\mathbf{r}_i + 2(\mathbf{r}_i\cdot\mathbf{r}_j)\mathbf{r}_j\right]. \qquad (3)$$

The physical libration of the moon P_i arises implicitly in the expression of $\nabla_0 U_{\bar{0}\bar{i}}$ and $\nabla_j U_{\bar{j}\bar{i}}$ in equations (1). For more details, the reader may refer to Lainey et al. (2019), equations (22) and (23).

The fitting process involved solving the variational equations for an unspecified parameter c_l of the model to be fitted (e.g. $\mathbf{r}(t_0), d\mathbf{r}/dt(t_0), Q$...); see Lainey (2016) for more details:

$$\frac{\partial}{\partial c_l}\left(\frac{d^2\mathbf{r}_i}{dt^2}\right) = \frac{1}{m_i}\left[\sum_j\left(\frac{\partial \mathbf{F}_i}{\partial \mathbf{r}_j}\frac{\partial \mathbf{r}_j}{\partial c_l} + \frac{\partial \mathbf{F}_i}{\partial \dot{\mathbf{r}}_j}\frac{\partial \dot{\mathbf{r}}_j}{\partial c_l}\right) + \frac{\partial \mathbf{F}_i}{\partial c_l}\right]. \qquad (4)$$

In the above expression, $\mathbf{F}_i$ is the right-hand side of Eq. (1) multiplied by m_i. The partial derivatives of the solutions with respect to initial positions and velocities of the satellites and dynamical parameters were then computed by the simultaneous numerical solution of Eqs. (1) and (4), in a Saturn-centred frame with inertial axes based on the Earth mean equator of J2000.

To test the reliability of our fit, we considered additional perturbations (see Tables **??**-**??**). Among other effects, we considered the influence of Mimas's extended gravity field, the Saturnian nutations from the SAT427 SPICE kernel (**?**)), the Saturnian polar orientation determined by French et al. (2017), the use of the SAT427 ephemerides for the main moons, and the influence of higher-order gravity parameters for the inner moons under the homogeneity assumption.

In summary, all our simulations involved solving simultaneously for the initial state vectors and masses of the moons, the masses and gravity field of Saturn, including zonal harmonics up to order 10, the orientation and precession of Saturn, and the physical librations for Prometheus, Pandora, Janus, and Epimetheus. No constraints were introduced in the fitting, except for Saturn's gravity field at the value estimated by Iess et al. (2019) assuming their published 1σ uncertainty.

2.2. Fitting the data

We used all astrometric data available for the moons ((Tajeddine et al. 2013) (Cooper et al. 2014); (Tajeddine et al. 2015); (Cooper et al. 2018);(Zhang et al. 2021); (Lainey et al. 2023);(Lainey et al. 2024)). To test tidal frequency Love number of k_2, we considered a two-step method. The first one solves for a constant k_2 and k_3. We obtained in that case $k_2 = ... \pm ..$ and $k_3 = ... \pm ..$ ($1\ \sigma$ error bar). In the second step, we solved for k_2 at all moons frequency. It turned out, that only four tidal frequencies could be fairly well constrained, which corresponds to tides associated with Janus and Epimetheus (being on an horsehoe orbit both moons share the same tidal frequency), Mimas, Tethys and Dione. In this second approach, we eventually introduced the constant k_2 and k_3 solution from the first approach for the other tidal frequencies.

From our second approach (non constant Love number k_2), we found out that the Love number values obtained for Janus/Epimetheus's, Tethys's and Dione's frequencies were obtained from cross tidal tidal effects, exactly in the same manner as already discovered by Lainey et al. (2017). On the other hand, the signal at Mimas's tidal frequency was determined thanks to its resonance with Pandora. Our estimation for the Saturnian Love number frequencies are ?? ± .. at Janus/Epimetheus's, Mimas's, Tethys's and Dione's tidal frequency, respectively.

3. Love number calculations

For comparison with the Love numbers fitted through dynamical modelling, we computed theoretical predictions using the numerical approach described in Dewberry (2023). Briefly, this method amounts to direct solution of Navier-Stokes, continuity, energy, and Poisson equations that have been linearized around an equilibrium, rotationally flattened model of Saturn, and subjected to an inhomogeneous tidal force assumed to have a harmonic time-dependence.

We computed Love numbers as a function of tidal frequency for two rigidly rotating, dilute core models of Saturn (we expect differential rotation from Saturn's zonal winds to have a marginal impact in this case): m23 is the best-fit model constrained by the ring seismological inference of Mankovich et al. (2023), and d21 is the model from Dewberry et al. (2021) with a dilute core extending over 72% of Saturn's equatorial radius. In order to resolve peaks associated with resonant oscillation modes (which are formally infinite in the absence of dissipation), we included a purely constant kinematic viscosity ν, and performed calculations for Ekman numbers $E_k = \nu/(\Omega_S R_S^2) = 10^{-5}, 10^{-6}$.

For the tidal driving, we approximated satellite tidal potentials as point-mass potentials expanded in spherical harmonics up to degree $\ell = 12$. We computed Love numbers k_{22} as the real part of the ratio Φ'_{22}/U_{22}, where U_{22} and Φ'_{22} are $\ell = m = 2$ coefficients in spherical harmonic expansions of the tidal potential and induced gravitational response (respectively). Including multiple harmonic degrees in the expansion of the tidal potential leads to some ambiguity in the definition of a response function defined for oblate bodies (since one spherical harmonic of the tidal potential can drive another in the response; Dewberry & Lai 2022), but this effect is minimal for sectoral ($\ell = m$) harmonics.

Table 1. Mean (ν) and standard deviation (σ) on sample and line in pixel for each satellite (Cassini-ISS data). N is the number of observations by satellite considered and for each coordinate. Observations with residuals higher than 2.5 pixels were discarded. NAC stands for the Narrow Angle Camera of the Cassini Imaging Science Subsystem.

Observations	ν_{sample} (pix)	σ_{sample} (pix)	ν_{line} (pix)	σ_{line} (pix)	N	satellite
ISS NAC (centroid fitting) prearrival	-0.2327	0.0000	0.8999	0.0000	1, 1	Titan
	-0.0404	0.2283	0.0866	0.1480	18, 18	Calypso
	0.0510	0.3000	0.0051	0.2042	21, 21	Telesto
	-0.0691	0.2381	0.0383	0.1657	11, 11	Helene
ISS NAC (MM centroid fitting) prearrival	-0.2527	0.1367	-0.1808	0.1945	11, 11	Atlas
ISS NAC (limb fitting)	0.0080	0.4883	0.1564	0.5422	155, 155	Mimas
	0.1015	0.6068	-0.0452	0.4768	1615, 1615	Enceladus
	-0.0764	0.3115	-0.0456	0.3164	452, 452	Tethys
	-0.0397	0.2794	0.0135	0.3003	752, 752	Dione
	-0.0916	0.3002	-0.0446	0.2608	649, 649	Rhea
	0.0696	1.7313	1.0702	1.4327	70, 70	Titan
	-0.0203	0.0969	0.8920	0.4051	3, 3	Hyperion
	-0.0511	0.6525	-0.0827	0.3566	80, 80	Iapetus
	0.0074	0.2576	-0.0725	0.2089	45, 45	Calypso
	-0.0656	0.2336	0.0220	0.1977	39, 39	Teltesto
	-0.0313	0.2527	-0.0375	0.2075	51, 51	Helene
	-0.0977	0.0770	0.0520	0.1059	3, 3	Pallene
ISS NAC (limb fitting) 3-d complex shape	0.0049	0.6912	0.1088	0.6991	166, 166	Atlas
	-0.0464	0.5251	-0.0664	0.5855	749, 749	Prometheus
	-0.0438	0.4417	-0.0693	0.5717	664, 664	Pandora
	-0.0349	0.3714	-0.1060	0.4758	532, 533	Epimetheus
	-0.0339	0.3552	-0.0692	0.4107	513, 513	Janus
ISS NAC (MM centroid fitting)	-0.0048	0.4345	-0.0722	0.3615	333, 333	Atlas
	-0.0110	0.1464	0.0067	0.1613	207, 207	Polydeuces
	0.0168	0.1752	-0.0215	0.2293	234, 234	Methone
	0.0005	0.1446	-0.0125	0.1316	169, 169	Anthe
ISS NAC green filter	-0.7505	1.0391	0.0077	0.7429	9, 9	Mimas
	0.3722	0.6972	0.2170	0.6830	49, 49	Tethys
ISS NAC red filter	-0.3327	0.0000	0.4694	0.0000	1, 1	Mimas
	0.2773	0.7195	0.5362	0.9669	11, 11	Tethys
ISS WAC (limb fitting)	-1.3335	0.0000	-0.0224	0.0000	1, 1	Mimas
	0.0863	0.0000	-0.7641	0.0000	1, 1	Dione
	0.2845	0.2258	0.2854	0.3724	2, 2	Rhea
	0.0372	0.0720	-0.2722	0.1168	4, 4	Calypso
	0.0749	0.1673	-0.1616	0.0895	6, 6	Telesto
	0.1602	0.1142	-0.2466	0.0567	2, 2	Helene
ISS NAC (limb fitting)	-0.0633	0.6675	-0.0027	0.3052	87, 87	Mimas
	0.0196	0.3406	0.1879	0.3616	36, 36	Tethys
ISS NAC green filter	-0.2658	0.6683	-0.1023	0.2637	19, 19	Mimas
	0.0382	0.3930	0.1385	0.3006	69, 69	Tethys
ISS NAC infra-red filter	-0.2092	0.8730	-0.0240	0.4375	19, 19	Mimas
	0.0177	0.3958	0.2544	0.5941	28, 28	Tethys
ISS NAC (limb fitting)	0.0359	0.9675	0.1487	0.5323	106, 106	Mimas
	-0.2353	0.3676	0.1374	0.3083	38, 38	Tethys
ISS NAC infra-red filter (limb fitting)	0.2662	0.4515	-0.4825	0.5388	4, 4	Mimas
	0.3280	0.7415	0.2231	0.5586	26, 26	Tethys

4. Conclusion

We were able to quantify Saturn's Love number, k_2, at four different tidal frequencies. This turns out to be compatible with a constant behavior within the error bars of the observations. This is in reasonable agreement with what is predicted by numerical models of inertial wave excitations in Saturn.

References

Cooper, N. J., Lainey, V., Meunier, L. E., et al. 2018, A&A, 610, A2
Cooper, N. J., Murray, C. D., Lainey, V., et al. 2014, A&A, 572, A43
Dewberry, J. W. 2023, MNRAS, 521, 5991
Dewberry, J. W. & Lai, D. 2022, ApJ, 925, 124
Dewberry, J. W., Mankovich, C. R., Fuller, J., Lai, D., & Xu, W. 2021, , 2, 198
French, R. G., McGhee-French, C. A., Lonergan, K., et al. 2017, Icarus, 290, 14
Iess, L., Militzer, B., Kaspi, Y., et al. 2019, Science, 364, aat2965
Lainey, V. 2016, Celestial Mechanics and Dynamical Astronomy, 126, 145
Lainey, V., Dehant, V., & Pätzold, M. 2007, A&A, 465, 1075
Lainey, V., Jacobson, R. A., Tajeddine, R., et al. 2017, Icarus, 281, 286
Lainey, V., Noyelles, B., Cooper, N., et al. 2019, Icarus, 326, 48
Lainey, V., Rambaux, N., Cooper, N., Dahoumane, R., & Zhang, Q. 2023, A&A, 670, L25
Lainey, V., Rambaux, N., Tobie, G., et al. 2024, Nature
Mankovich, C. R., Dewberry, J. W., & Fuller, J. 2023, , 4, 59
Newhall, X. X., Standish, E. M., & Williams, J. G. 1983, A&A, 125, 150
Tajeddine, R., Cooper, N. J., Lainey, V., Charnoz, S., & Murray, C. D. 2013, A&A, 551, A129
Tajeddine, R., Lainey, V., Cooper, N. J., & Murray, C. D. 2015, A&A, 575, A73
Zhang, Q. F., Zhou, X. M., Tan, Y., et al. 2021, MNRAS, 505, 5253

Table 2. Mean (ν) and standard deviation (σ) on sample and line in pixel for each satellite (Cassini-ISS data). N is the number of observations by satellite considered and for each coordinate. Observations with residuals higher than 2.5 pixels were discarded. NAC stands for the Narrow Angle Camera of the Cassini Imaging Science Subsystem.

Observations	ν_{sample} (pix)	σ_{sample} (pix)	ν_{line} (pix)	σ_{line} (pix)	N	satellite
ISS NAC (centroid fitting)	-0.0185	0.1947	-0.0499	0.2023	356, 356	Calypso
	-0.0329	0.1875	-0.0320	0.2573	360, 360	Telesto
	0.0112	0.2572	-0.1156	0.2695	322, 322	Helene
	-0.0091	0.2719	-0.0498	0.2394	279, 279	Pallene
ISS NAC red filter (limb fitting)	-0.9507	0.5119	0.0475	0.1209	4, 4	Mimas
	0.2170	0.5048	0.0704	0.2873	32, 32	Tethys
ISS NAC infra-red filter (limb fitting)	2.3577	0.1035	0.4656	0.3062	2, 2	Mimas
ISS NAC (limb fitting)	0.4281	0.1584	-0.1455	0.0494	2, 2	Dione
	1.1336	0.0000	0.1581	0.0000	1, 1	Iapetus

Table 3. Statistics of the ISS-NAC astrometric residuals computed in km. ν and σ denote respectively the mean and standard deviation of the residuals computed on RA and DEC. N columns are the number of observations considered for the respective coordinate.

Observations	ν_{sample} (km)	σ_{sample} (km)	ν_{line} (km)	σ_{line} (km)	N	satellite
ISS NAC (limb fitting from free ellipse)	-1.3199	3.1132	-0.1538	2.7952	743, 743	Mimas
	-0.7422	3.2694	0.9055	3.0855	920, 920	Enceladus
	-0.4708	4.3961	0.7415	3.7807	922, 923	Tethys
	-0.1254	3.1857	0.3505	3.3475	1324, 1328	Dione
	-0.7188	3.0943	0.4697	2.8552	1345, 1347	Rhea
	-0.0777	12.6786	2.7285	10.1644	72, 88	Hyperion
	1.3099	5.3232	-1.1750	5.2649	1533, 1533	Iapetus

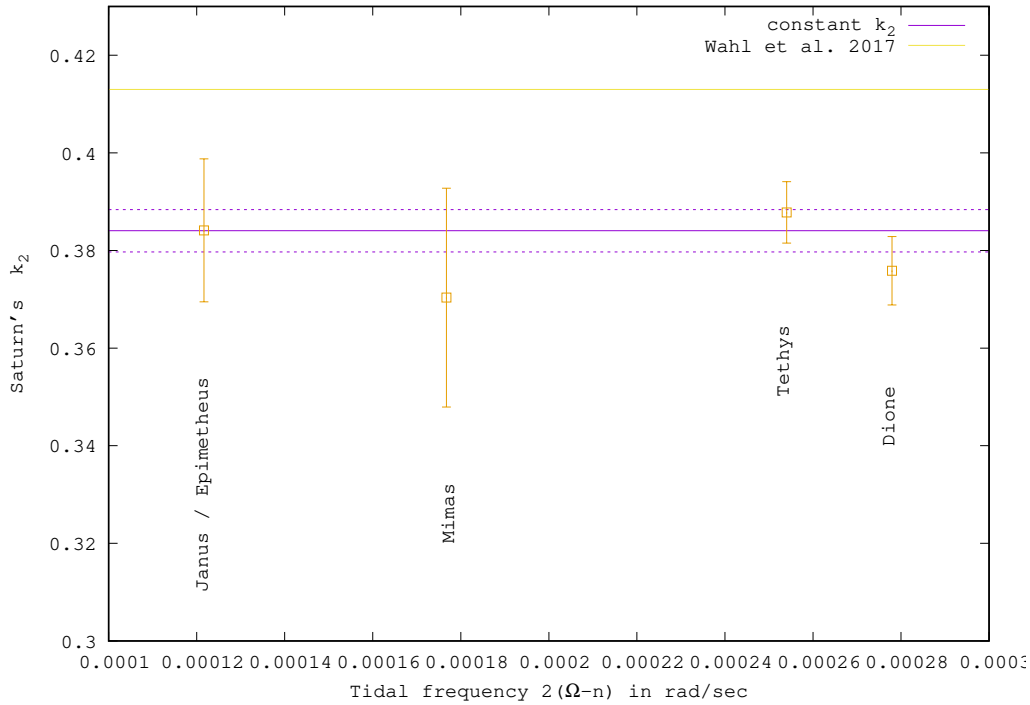

Fig. 1. Frequency variation of the Saturnian Love number k_2 from astrometric data.

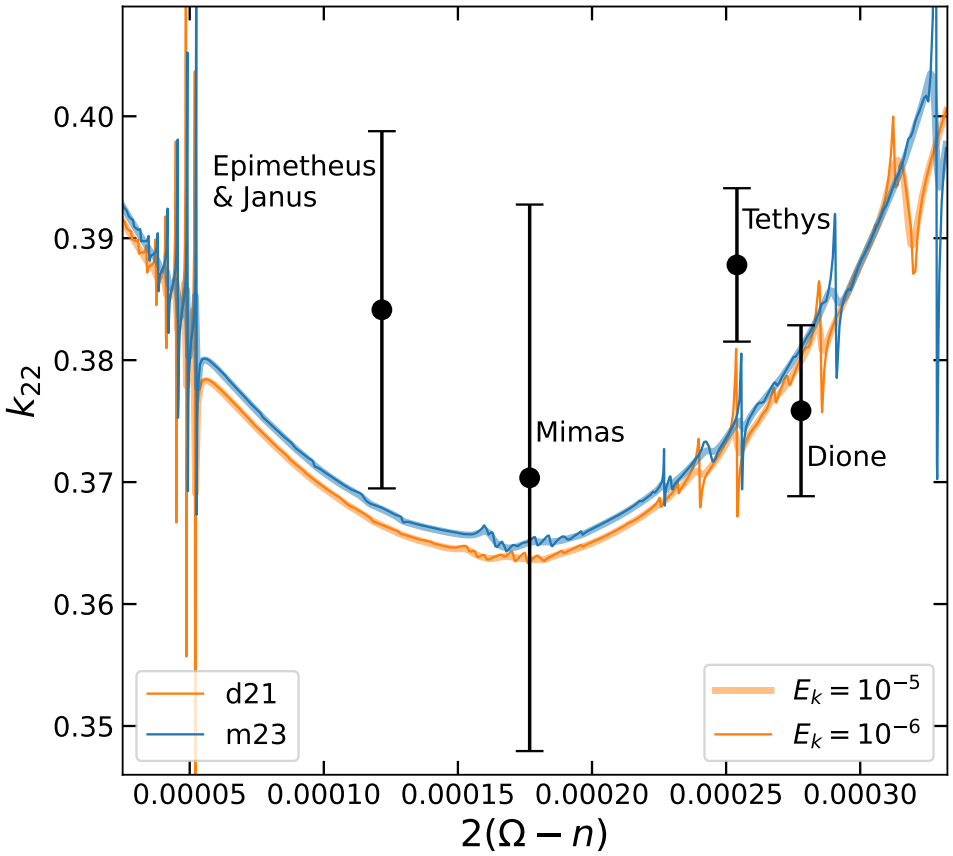
0.40
0.39
0.38
0.37
0.36
0.35
k_{22}
Epimetheus
& Janus
Mimas
Tethys
Dione
d21
m23
$E_k = 10^{-5}$
$E_k = 10^{-6}$
0.00005
0.00010
0.00015
0.00020
0.00025
0.00030
$2(\Omega - n)$

Fig. 2.